Thermochimica Acta 471 (2008) 51–54

Contents lists available at ScienceDirect

Thermochimica Acta

journal homepage: www.elsevier.com/locate/tca

TPR/TPO characterization of cobalt–silicon mixed oxide nanocomposites prepared by sol–gel

Giovanni Bagnasco[a,*], Claudia Cammarano[a], Maria Turco[a], Serena Esposito[b], Antonio Aronne[c], Pasquale Pernice[c]

[a] Università di Napoli Federico II, Dipartimento di Ingegneria Chimica, Piazzale Tecchio, 80125 Napoli, Italy
[b] Università di Cassino, Dipartimento di Meccanica, Strutture, Ambiente e Territorio, Via G. di Biasio 43, 03043 Cassino, Italy
[c] Università di Napoli Federico II, Dipartimento di Ingegneria dei Materiali e Produzione, Piazzale Tecchio, 80125 Napoli, Italy

ARTICLE INFO

Article history:
Received 7 December 2007
Received in revised form 22 February 2008
Accepted 27 February 2008
Available online 4 March 2008

Keywords:
TPR/TPO
Cobalt–silicon mixed oxides
Sol–gel method

ABSTRACT

Cobalt–silicon mixed oxides with Co/Si ratio of 10/90 (10Co), 20/80 (20Co) and 30/70 (30Co) were prepared by a modified sol–gel method. The materials treated in air at 400 and 600 °C were characterized by SEM and TPR/TPO techniques. TPR measurements showed that in all samples only a fraction of Co was present as Co_3O_4 and as amorphous silicate and was reducible by H_2 within 800 °C, while a part was not reducible under TPR conditions. The fraction of Co not reducible decreased with increasing Co content. A TPO/TPR cycle gave rise to an increase of the fraction of not reducible Co.

1. Introduction

Cobalt/silica systems are widely studied as gas sensors [1] or catalysts for many reactions involving hydrogen transfer, such as methane reforming [2–4], hydrogenation of aromatics [5], selective hydrogenation of α,β-unsaturated aldehydes [6], epoxidation of olefins [7], methanol dehydrogenation [8] and especially the Fischer-Tropsch synthesis (FTS) [9–11]. The last process is forecasted to gain importance in the near future for the conversion of biomasses to liquid biofuels, according to EU targets of increasing use of renewable energy sources [12,13].

Among different synthesis methods, such as impregnation [5,14–16], precipitation [14,17], grafting [18], the sol–gel has the advantage of a better control of the microstructure and texture of the silica matrix [19–22] and allows a more effective dispersion of cobalt oxide in the silica matrix [7]. Catalytic properties of the metallic Co^0 phase are strongly influenced by the nature of Co compounds present in the precursor materials before their reduction to Co^0 [16]. When Co is present in the precursor mainly as the oxide Co_3O_4, the reduction with H_2 can be obtained at a relatively low temperature, thus producing a well-dispersed and highly active Co^0 phase. On the other hand, if Co is present as Co silicates, very high temperatures are required for reduction, thus producing a less dispersed and less active Co^0 phase [17]. The use of an easily hydrolysable Co salt, such as Co acetate, and the presence of a high concentration of water vapor during the heat treatment favor the formation of Co hydroxide and its following reaction with silicic acid producing Co silicate. Decomposition of the Co salt at high temperature and heat treatment in a reducing atmosphere also favor the formation of undesired Co silicates [14,16,23].

In a previous work highly dispersed cobalt–silicon mixed oxide nanocomposites were synthesized by a modified sol–gel method and were characterized by different techniques [24]. The nature of cobalt species was strongly depending on both the cobalt loading and the heat treatment. The materials appeared very promising as catalyst precursors due to the high dispersion of Co species and formation of crystalline Co_2SiO_4 only at high temperatures. In view of a possible application as catalysts, the study of redox properties of such materials deserves a special attention, therefore they are investigated in the present work by means of TPR and TPO techniques. TPR, eventually coupled with O_2 titration, appeared an effective technique for the characterization of redox properties of Co/SiO_2 systems [6,9,15,16,25].

2. Experimental

Cobalt–silicon mixed oxides with Co/Si = 10/90 (10Co), 20/80 (20Co) and 30/70 (30Co) were prepared by sol–gel starting from

* Corresponding author. Tel.: +39 0817682259; fax: +39 0815936936.
E-mail address: bagnasco@unina.it (G. Bagnasco).

0040-6031/$ – see front matter © 2008 Elsevier B.V. All rights reserved.
doi:10.1016/j.tca.2008.02.019

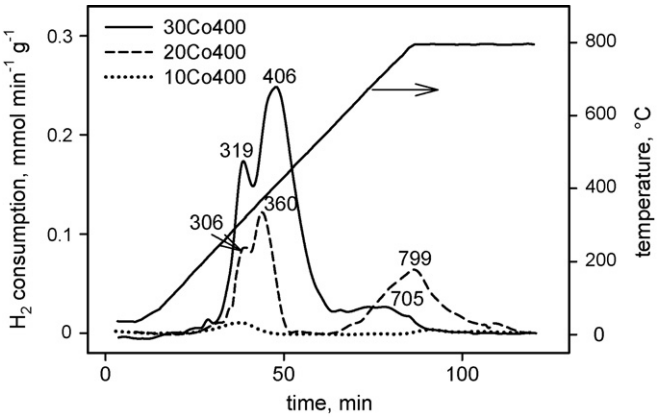

Fig. 1. TPR spectra of samples treated at 400 °C.

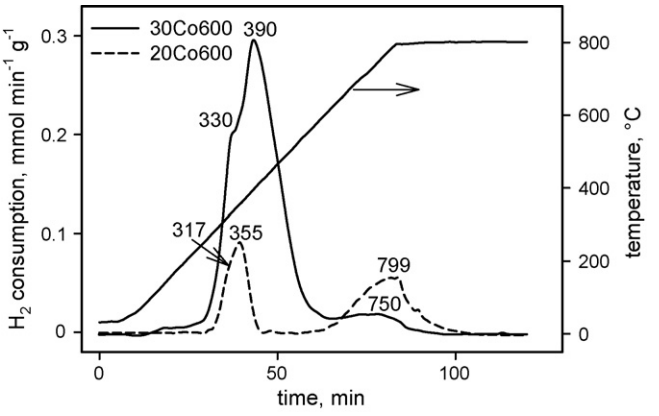

Fig. 2. TPR spectra of samples treated at 600 °C.

$Co(NO_3)_2{\cdot}6H_2O$ (Acros Organics) and $Si(OC_2H_5)_4$ (99%, ABCR) without any alcoholic solvent, using nitric acid as catalyst. The gels were dried in air at 110 °C for 12 h and after calcined at 400 or 600 °C for 2 h. Details of the procedure are reported in a previous paper [24]. The samples are identified by the Co content followed by the temperature of heat treatment.

Pure silica gel derived glass was synthesized as reference material by hydrolyzing $Si(OC_2H_5)_4$ under the same conditions as described above.

TPR and TPO measurements were carried out in a laboratory flow apparatus, using a 5% H_2/Ar ($Q = 150\,cm^3\,min^{-1}$) or a 2% O_2/He mixture ($Q = 80\,cm^3\,min^{-1}$), respectively, with heating rate of 10 °C min^{-1} up to 800 °C. The sample (100 mg, size 75–90 μm) was loaded in a quartz down-flow cell with a K thermocouple in close contact with the sample. A chromatographic thermal conductivity detector connected to a data acquisition system was employed to record the composition of the effluent stream. H_2O that could interfere with the analysis was removed by an anhydrous KOH trap.

3. Results and discussion

TPR spectra of all samples treated at 400 °C are reported in Fig. 1. Reduction profile of 10Co400 shows very low intensity signals at 305 and 798 °C, while for the samples with higher Co content a couple of more evident peaks appear in the range 300–400 °C, followed by other signals at 700–800 °C. The peaks in the range 300–400 °C can be attributed to the two-step reduction of the oxide Co_3O_4, as suggested by many works on materials containing this compound in a dispersed form [6,9,15,19], although pure Co_3O_4 gives one TPR signal [26]. The high temperature signal at 700–800 °C can be related to reduction of Co^{2+} ions bonded to the siloxane framework [7,8,9,19]. These species can be regarded as amorphous Co silicate, showing similar redox properties, although the crystalline phase Co_2SiO_4 is formed only at much higher temperature, as observed previously [24]. The amounts of H_2 corresponding to the signals at 300–400 °C (low T) and 700–800 °C (high T) related to reduction of Co_3O_4 and Co in amorphous silicate, respectively, are calculated from the areas underlying TPR peaks and reported in Table 1. It is found that for every sample the amount of Co corresponding to the total H_2 consumption is less than the actual Co content, this means that there is a fraction of Co not reducible under the present conditions. The last three columns of Table 1 report the results of an estimation of the fractions of Co present as: (i) oxide Co_3O_4, (ii) amorphous silicate reduced at 700–800 °C and (iii) not reducible Co. The amount of Co_3O_4 is very low in the sample 10Co400 and increases with Co content, Co in amorphous silicate (the high temperature TPR signal) is maximum in the sample 20Co400, while the amount of not reducible Co is the highest for 10Co400.

These results agree with XRD measurements previously reported showing that the sample 10Co400 is amorphous, while crystalline Co_3O_4 is present in 20Co400 and 30Co400 in amounts increasing with Co content [24]. On the other hand, no crystalline Co silicate was detected by XRD in any of the samples treated at 400 °C: the Co_2SiO_4 phase was detected in all samples only after treatment at 850 °C [24]. This suggests that the TPR signals observed at 700–800 °C are related to an amorphous Co silicate. As regards the not reducible Co, this can be related to tetrahedral Co(II) that, being strongly bonded into the siloxane framework [24], cannot be reduced under the present conditions. The large fraction of not reducible Co in the sample 10Co400 can be explained by a stronger interaction of Co(II) with the siloxane matrix in comparison with the samples with higher Co content [24]. It could be also hypothesized that part of Co is inaccessible to H_2.

The TPR profiles of the samples treated at 600 °C in air flow are depicted in Fig. 2, while the corresponding amounts of H_2 consumed are reported in Table 2.

The spectrum of 10Co600 is not reported because the TPR signals of this sample are below the sensitivity limit of the apparatus. Also in this case, two types of signals can be noted, those with maxima between 300 and 400 °C, that can be attributed to the reduction of the oxide Co_3O_4, and those at 700–800 °C related to Co in the amorphous silicate phase. However some small differences are observed in comparison with the spectra of samples treated at 400 °C.

This effect is probably due to some structural changes that occur between 400 and 600 °C, mainly a further polycondensation of

Table 1
Results of TPR measurements for samples treated at 400 °C

Sample	T_{max} (°C)	H_2 consumption (mmol g^{-1})		Co distribution (%)		
		Low T	High T	Co_3O_4	Co silicate	Not reduced
10Co400	305, 798	0.14	0.09	6.5	5.5	88.0
20Co400	306, 360, 799	1.33	1.54	33.3	50.0	16.7
30Co400	319, 406, 705	4.50	0.52	75.1	11.5	13.4

Table 2
Results of TPR measurements for samples treated at 600 °C

Sample	T_{max} (°C)	H_2 consumption (mmol g^{-1})		Co distribution (%)		
		Low T	High T	Co_3O_4	Co silicate	Not reduced
20Co600	317(sh), 355, 799	0.65	1.19	15.7	38.4	45.9
30Co600	330(sh), 390, 750	4.57	0.43	76.3	9.5	14.2

Table 3
H_2 and O_2 consumed in the TPR/TPO/TPR cycle

Sample	I TPR, H_2 (mmol g^{-1})	TPO, O_2 (mmol g^{-1})	II TPR, H_2 (mmol g^{-1})
20Co400	2.87	0.95	1.66
30Co400	5.02	2.15	3.95

silanol groups [24] that however are not detectable by XRD analysis. From the values of H_2 consumed (Table 2) it can be noted that the 30Co600 behaves like the sample 30Co400, while the sample 20Co600 shows a decrease of the amounts of Co_3O_4 and Co in amorphous silicate in comparison with the 20Co400, with the consequent increase of the fraction of not reducible Co. This indicates that treating at higher temperature the amount of Co strongly bonded into the siloxane framework or inaccessible to H_2 increases. In order to obtain more information on the degree of reduction and the properties of the metallic Co phase, a TPO/TPR cycle was carried out on the samples 20Co400 and 30Co400 after the first TPR test.

TPO profiles, reported in Fig. 3, show that for both samples the re-oxidation is a complex process occurring in more than one step, probably due to the presence of Co metallic particles of different sizes. However the two samples show a very different behavior: the sample 30Co400 is oxidized at lower temperature, suggesting the presence of a more dispersed metallic phase. According to the results reported in a previous work [24], in these materials the Co_3O_4 phase is highly dispersed, with particles dimension of about 13 nm. The reduction of such a nanosized phase produces highly dispersed metallic Co [27,28]. The sample 30Co400, containing a higher amount of Co in the form of Co_3O_4, gives rise to a more dispersed Co^0 after TPR.

TPR spectra obtained after TPO tests are shown in Fig. 4. Compared with the results of TPR tests on fresh materials (Fig. 1), these profiles also point to the presence of Co_3O_4 and amorphous Co silicate, but the different shapes of the peaks indicate some structural differences. The peaks are more tailed, suggesting a slower reduction process, probably related to diffusion effects. It is possible that the redox cycle involving high temperature heating has reduced the porosity of the materials, and this increases diffusion resistances. A lower diffusion rate increases the residence time of water vapour in the pores, causing a longer tailing of TPR peaks. A similar effect was hypothesized for supported Co/SiO_2 catalysts [22]. The amounts of H_2 and O_2 consumed during the steps of the redox cycle are reported in Table 3. From these data, it can be noted that the amount of O_2 consumed during TPO is less than that expected on the basis of the amount of H_2 consumed in the previous TPR test (a O_2/H_2 ratio slightly higher than 0.5 is expected, since part of Co^0 derives from Co_3O_4 and part from amorphous cobalt silicate in which Co is probably in the oxidation state 2+). This is specially true for the sample 20Co400 and can be due to different factors. An incomplete oxidation of Co can be explained by partial collapse of the siloxane matrix around the metal particles that hinders the Co oxidation: a similar effect of encapsulation was observed for supported Co/SiO_2 catalysts reduced at temperature higher than 500 °C [5]. Moreover it is possible that during the TPO tests, a part of cobalt oxide produced reacts with the siloxane matrix forming a Co(II) silicate instead of Co_3O_4, thus consuming a lower amount of O_2.

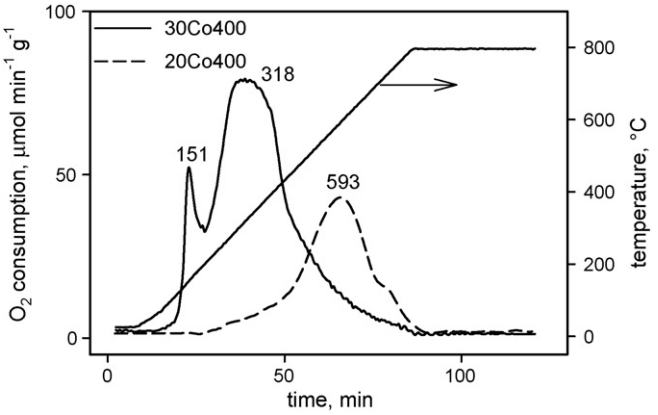

Fig. 3. TPO spectra of 20Co400 and 30Co400 after TPR tests.

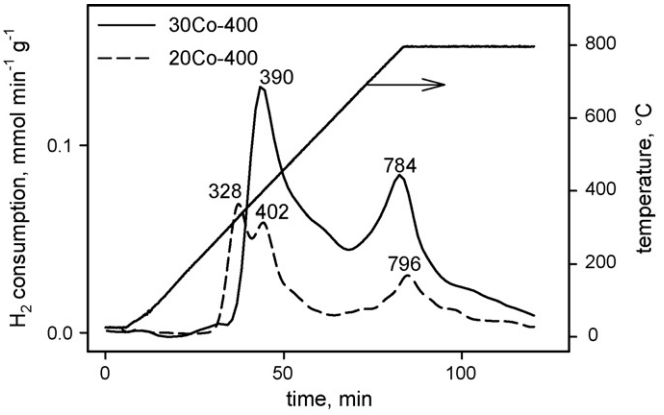

Fig. 4. TPR spectra of 20Co400 and 30Co400 after TPO tests.

As regards the TPR tests following TPO, it is noted from Table 3 that the amounts of H_2 consumed are much smaller than those related to the first TPR: moreover they are also smaller than the stoichiometric ones corresponding to the previous TPO tests. A possible explanation of this behaviour can be that during the TPO tests, some Co(II) has reacted with the siloxane matrix, producing further amounts of unreducible Co. Again this effect is more evident for the 20Co400, confirming that any chemical interaction between Co species and the siloxane matrix is favored at lower Co loading. It must be supposed that Co(II) continues to react with the siloxane matrix whenever the temperature is raised, as such behaviour was seen also on similar materials prepared by impregnation method [8].

4. Conclusions

The TPR/TPO technique has proved effective to characterize different Co species present in cobalt–silicon mixed oxide nanocomposites prepared by sol–gel. Significant differences were evidenced in the redox properties of heat-treated materials depending on their chemical composition. TPR signals allowed to evaluate the amounts of the different Co species: spinel oxide Co_3O_4 and amorphous silicate. The last was present in all samples, while Co_3O_4 was present in appreciable amounts in the samples with high Co content. A fraction of cobalt amorphous silicate strongly interacting with the siloxane matrix was not reducible under the present TPR conditions.

References

[1] C. Cantalini, M. Post, D. Buso, M. Guglielmi, A. Martucci, Sens. Actuators B 108 (2005) 184.
[2] R. Bouarab, O. Akdim, A. Auroux, O. Cherifi, C. Mirodatos, Appl. Catal. A: Gen. 264 (2004) 161.
[3] W.K. Jozwiak, E. Szubiakiewicz, J. Goralski, A. Klonkowski, T. Paryjczak, Kinet. Catal. 45 (2004) 247.
[4] E. Ruckenstein, H.Y. Wang, Appl. Catal. A: Gen. 204 (2000) 257.
[5] J.M. Jabłonski, J. Okal, D. Potoczna-Petru, L. Krajczyk, J. Catal. 220 (2003) 146.
[6] F. Djerboua, D. Benachour, R. Touroude, Appl. Catal. A: Gen. 282 (2005) 123.
[7] M.L. Kantam, B.P.C. Rao, R.S. Reddy, N.S. Sekhar, B. Sreedhar, B.M. Choudary, J. Mol. Catal. A: Chem. 272 (2007) 1.
[8] M.S. Ghattas, Micropor. Mesopor. Mater. 97 (2006) 107.
[9] T. Mochizuki, T. Hara, N. Koizumi, M. Yamada, Appl. Catal. A: Gen. 317 (2007) 97.
[10] T.K. Das, W.A. Conner, J. Li, G. Jacobs, M.E. Dry, B.H. Davis, Energy Fuels 19 (2005) 1430.
[11] A. Martinez, C. Lopez, F. Marquez, I. Diaz, J. Catal. 220 (2003) 486.
[12] L. Plass, S. Reimelt, Chem. Ing. Tech. 79 (2007) 561.
[13] H. Boerrigter, A. van der Drift, DGMK Tagungs Ber. 2 (2006) 49.
[14] I. Puskas, T.H. Fleisch, P.R. Full, J.A. Kaduk, C.L. Marshall, B.L. Meyers, Appl. Catal. A: Gen. 311 (2006) 146.
[15] D. Song, J. Li, J. Mol. Catal. A: Chem. 247 (2006) 206.
[16] J.-S. Girardon, A.S. Lermontov, L. Gengembre, P.A. Chernavskii, A. Griboval-Constant, A.Y. Khodakov, J. Catal. 230 (2005) 339.
[17] G.L. Bezemer, P.B. Radstake, V. Koot, A.J. van Dillen, J.W. Geus, K.P. de Jong, J. Catal. 237 (2006) 291.
[18] L. Guillou, D. Balloy, Ph. Supiot, V. Le Courtois, Appl. Catal. A: Gen. 324 (2007) 42.
[19] B.C. Dunn, P. Cole, D. Covington, M.C. Webster, R.J. Pugmire, R.D. Ernst, E.M. Eyring, N. Shah, G.P. Huffman, Appl. Catal. A: Gen. 278 (2005) 233.
[20] K. Okabe, X. Li, T. Matsuzaki, H. Arakawa, K. Fujimoto, J. Sol–Gel Sci. Technol. 19 (2000) 519.
[21] K. Okabe, X. Li, M. Wei, H. Arakawa, Catal. Today 89 (2004) 431.
[22] B. Ernst, S. Libs, P. Chaumette, A. Kiennemann, Appl. Catal. A: Gen. 186 (1999) 145.
[23] J.M. Jabłonski, M. Wolcirz, L. Krajczyk, J. Catal. 173 (1998) 530.
[24] S. Esposito, M. Turco, G. Ramis, G. Bagnasco, P. Pernice, C. Pagliuca, M. Bevilacqua, A. Aronne, J. Solid State Chem. 180 (12) (2007) 3341.
[25] S. Storsæter, B. Tødtal, J.C. Walmsley, B.S. Tanem, A. Dolmen, J. Catal. 236 (2005) 139.
[26] Q. Tang, Q. Zhang, H. Wu, Y. Wang, J. Catal. 230 (2005) 384.
[27] J.-S. Girardon, E. Quinet, A. Griboval-Constant, P.A. Chernavskii, L. Gengembre, A.Y. Khodakov, J. Catal. 248 (2007) 143.
[28] P.A. Chernavskii, A.Y. Khodakov, G.V. Pankina, J.-S. Girardon, E. Quinet, Appl. Catal. A: Gen. 306 (2006) 108.